

## Development of *Toxoplasma gondii* Calcium-Dependent Protein Kinase 1 (TgCDPK1) Inhibitors with Potent Anti-*Toxoplasma* Activity<sup>†</sup>

Steven M. Johnson,<sup>‡</sup> Ryan C. Murphy,<sup>‡</sup> Jennifer A. Geiger,<sup>⊥</sup> Amy E. DeRocher,<sup>⊥</sup> Zhongsheng Zhang,<sup>||</sup> Kayode K. Ojo,<sup>§</sup> Eric T. Larson,<sup>||</sup> B. Gayani K. Perera,<sup>‡</sup> Edward J. Dale,<sup>‡</sup> Panqing He,<sup>§</sup> Molly C. Reid,<sup>§</sup> Anna M. W. Fox,<sup>§</sup> Natascha R. Mueller,<sup>§</sup> Ethan A. Merritt,<sup>||</sup> Erkang Fan,<sup>||</sup> Marilyn Parsons,<sup>⊥, #</sup> Wesley C. Van Voorhis,<sup>\*, §, #</sup> and Dustin J. Maly<sup>\*, ‡</sup>

<sup>‡</sup>Department of Chemistry, University of Washington, Seattle, Washington, United States

<sup>§</sup>Department of Medicine, Division of Allergy and Infectious Diseases, University of Washington, Seattle, Washington, United States

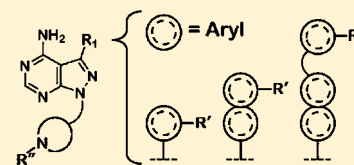
<sup>||</sup>Department of Biochemistry, University of Washington, Seattle, Washington, United States

<sup>⊥</sup>Seattle Biomedical Research Institute, Seattle, Washington, United States

<sup>#</sup>Department of Global Health, University of Washington, Seattle, Washington, United States

### **S** Supporting Information

**ABSTRACT:** Toxoplasmosis is a disease of prominent health concern that is caused by the protozoan parasite *Toxoplasma gondii*. Proliferation of *T. gondii* is dependent on its ability to invade host cells, which is mediated in part by calcium-dependent protein kinase 1 (CDPK1). We have developed ATP competitive inhibitors of TgCDPK1 that block invasion of parasites into host cells, preventing their proliferation. The presence of a unique glycine gatekeeper residue in TgCDPK1 permits selective inhibition of the parasite enzyme over human kinases. These potent TgCDPK1 inhibitors do not inhibit the growth of human cell lines and represent promising candidates as toxoplasmosis therapeutics.



### ■ INTRODUCTION

*Toxoplasma gondii* is a food and waterborne pathogen that can infect humans and all warm-blooded animals.<sup>1,2</sup> It is acquired by consumption of undercooked meat bearing tissue cysts or by ingesting foods or water contaminated with oocysts shed by infected felines. The oocysts are highly infectious and environmentally stable, making infection by this route a serious concern in areas where the water supply is not safe and secure. During the initial infection, the parasites proliferate rapidly as tachyzoites until controlled by the immune system. At that point, the parasite transforms into the bradyzoite, a slow growing stage, establishing a reservoir of tissue cysts in the brain and other tissues. Periodically, the tissue cysts rupture, releasing tachyzoites that again replicate rapidly. If not brought under control by the immune system, this can cause re-emergence of the disease. The result in immunocompromised individuals is toxoplasmic encephalitis. In some regions of the world, *T. gondii* infections even appear to be problematic in immunocompetent individuals, such as foci in Brazil where up to 17% of individuals suffer from ocular toxoplasmosis<sup>3</sup> and in French Guiana where severely life-threatening manifestations of infection have been seen in immunocompetent patients.<sup>4</sup> A recent study suggests that a large fraction of individuals with ocular toxoplasmosis also have tachyzoites in the blood.<sup>5</sup> When initial infection with *T. gondii* occurs during pregnancy, it can be vertically transmitted, often leading to birth defects or miscarriage. A recent review of the literature illuminates the high prevalence of *T. gondii* infection in women of childbearing

age.<sup>6</sup> Approximately 11% of the U.S. population is seropositive for *T. gondii*, with most studies of European populations reporting 20–35% seropositivity.<sup>1,7</sup> In less developed countries, these rates can reach 50–75%.<sup>6</sup> Thus, many individuals who become immunocompromised are at risk for developing acute toxoplasmosis.

In immunocompetent individuals, toxoplasmosis is usually asymptomatic but can appear as mild flulike symptoms in some instances. For these individuals, recovery usually occurs without antimicrobial treatment. However, the fact that toxoplasma infection is epidemiologically associated with schizophrenia suggests that some immunocompetent individuals may also suffer from other adverse health effects.<sup>8</sup> For immunocompromised individuals, intensive treatment is often required for the infection, with additional suppressive therapy necessary for the duration of the immunosuppression. This treatment can be for life in the case of patients with AIDS, though with immune reconstitution after highly active antiretroviral therapy, suppressive treatment can be stopped. Before the era of highly effective antiretrovirals, toxoplasmic encephalitis was the initial AIDS-defining illness in up to 33% of cases.<sup>9</sup> First line therapy for toxoplasmosis typically involves a combination regimen of pyrimethamine with a sulfa (sulfonamide) drug, such as sulfadiazine.<sup>2</sup> For patients with sensitivity to sulfa drugs, clindamycin can be administered in lieu of sulfadiazine.

Received: December 20, 2011

Published: February 9, 2012

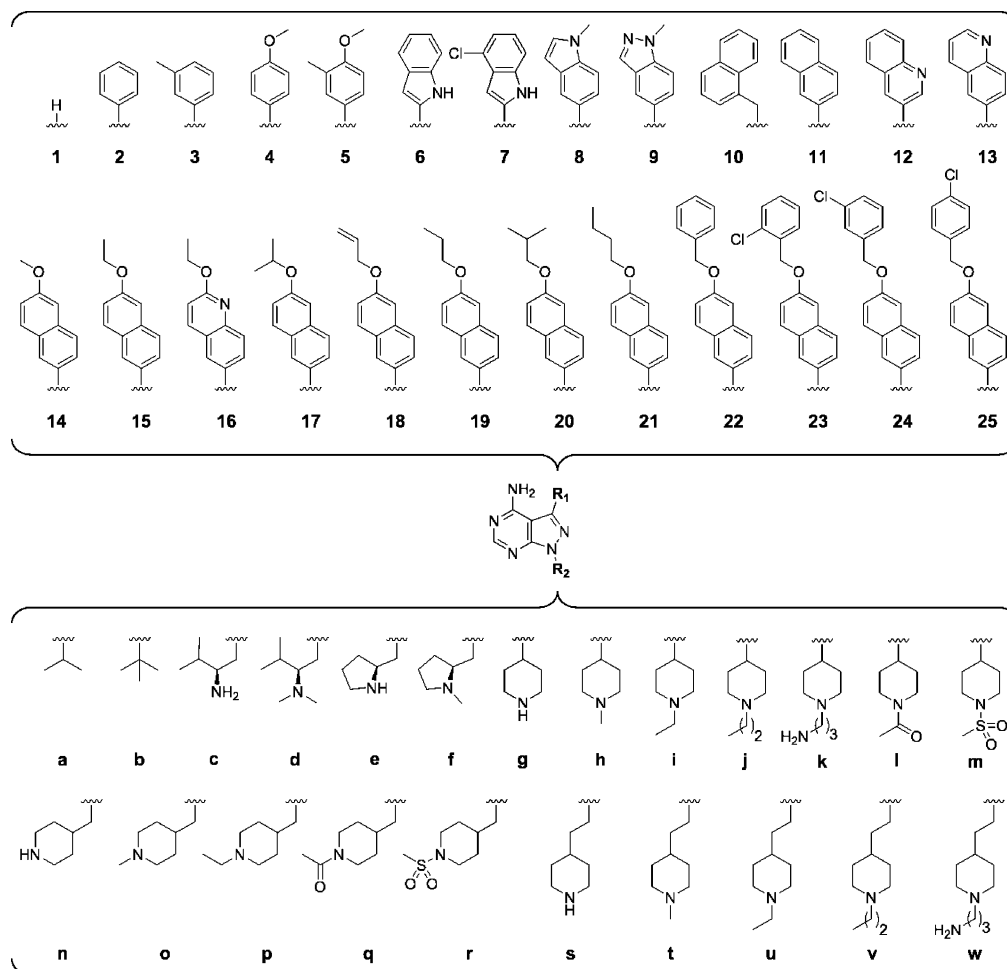
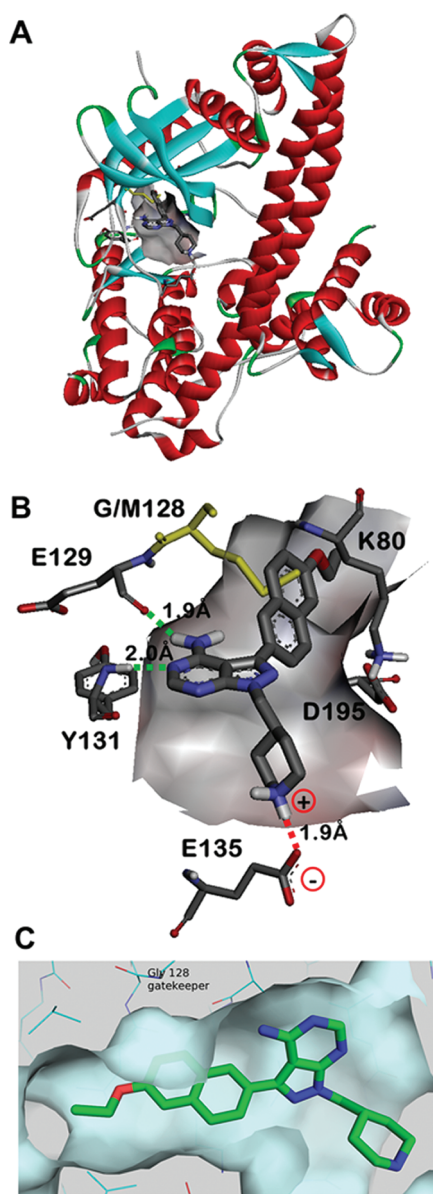


Figure 1.  $R_1$  and  $R_2$  substructures of compounds evaluated in this study.

Leucovorin (folinic acid) is coadministered to mitigate the toxic effects that pyrimethamine has on bone marrow. Additionally, pyrimethamine is teratogenic and is thus contraindicated for use in women during their first trimester of pregnancy. While not as effective as pyrimethamine and sulfonamides, spiramycin is recommended in these circumstances and has proven moderately effective at reducing congenital transmission.<sup>2,10,11</sup> Unfortunately, spiramycin has yet to gain FDA approval in the United States. While other *T. gondii* antiparasitic drugs are available, these agents also have significant drawbacks. Because of the toxicity associated with current toxoplasmosis therapeutics, complicated dosing regimens, and decreased effectiveness of second-line treatments when pyrimethamine and sulfonamides are contraindicated, there is the need to develop new *T. gondii* antiparasitic drugs that are nontoxic to humans and possess simpler dosing profiles.

In developing new toxoplasmosis therapeutics, we are exploring enzyme targets that are involved in calcium-regulated biological processes, such as host cell invasion, gliding motility, and exocytosis.<sup>12,13</sup> A key component of the signaling pathways that regulate these events is the calcium-dependent protein kinase CDPK1. As calcium levels increase, CDPK1 is activated, leading to increased gliding and motility, which is important for both parasite invasion and egress.<sup>14</sup> Because *T. gondii* is an obligate intracellular parasite that requires invasion of mammalian host cells to proliferate, *TgCDPK1* represents a

promising drug target for the development of antiparasitic agents. We previously developed several ATP-competitive inhibitors of *TgCDPK1* enzymatic activity and confirmed that *TgCDPK1* inhibition prevents invasion of *T. gondii* into host cells, blocking parasite proliferation.<sup>15,16</sup> A critical consideration of this antiparasitic strategy is to minimize perturbation of off-target mammalian signaling pathways by selectively targeting *TgCDPK1* over the 518 kinases present in humans. We were able to accomplish this goal by exploiting a unique sequence and structural variation in the ATP-binding cleft of *TgCDPK1*, where the presence of a small glycine gatekeeper residue permits large hydrophobic substituents displayed from the C-3 position of the pyrazolopyrimidine scaffold to occupy an adjacent hydrophobic pocket (Figures 1 and 2). Human kinases contain gatekeeper residues with larger side chains that sterically occlude access to this pocket. On the basis of structure–activity relationships from our previous studies,<sup>15,16</sup> we have developed an optimized panel of *TgCDPK1* inhibitors. Numerous compounds from this panel are extremely potent inhibitors of *TgCDPK1* activity in vitro and block *T. gondii* host cell invasion and proliferation. Several lead candidates were further shown to be highly selective for *TgCDPK1* over a panel of human kinases and additionally do not inhibit the growth of human cell lines, suggesting that this antiparasitic strategy could prove to be nontoxic to mammalian systems.



**Figure 2.** X-ray crystallographic structure of compound **15n** bound to wild type *T. gondii* CDPK1 (PDB accession code: 3SX9).<sup>18</sup> (A) Complete view of the **15n**-TgCDPK1 cocrystal structure. (B) Expanded view of the ATP binding site from part A (protein backbone ribbons have been removed for clarity). The backbone carbonyl of Glu129 and NH of Tyr131 hydrogen-bond with the exocyclic amine and adjacent endocyclic nitrogen of the pyrazolopyrimidine core, respectively (green dashed lines). The Glu135 side chain carboxylate makes a solvent exposed salt bridge with the piperidine R<sub>2</sub> ring, which is protonated under physiological conditions (red dashed line). The R<sub>1</sub> aryl substructure is oriented toward the Gly128 gatekeeper residue and into the adjacent hydrophobic pocket. The mutant Met128 residue (yellow) has been overlaid to show the steric clash that would occur between a larger gatekeeper side chain with the inhibitor R<sub>1</sub> substructures. The catalytic Lys80 and Asp195 side chains are also shown for context. (C) Rotated side/bottom view of the ATP binding site from part B.

## RESULTS AND DISCUSSION

**Molecular Design and Synthesis.** We have previously shown that pyrazolopyrimidine-based molecules, variably substituted at the R<sub>1</sub> and R<sub>2</sub> positions of the core scaffold (Figure 1), are potent inhibitors of TgCDPK1 enzymatic

activity.<sup>16</sup> In that study, two distinct molecular series were developed to optimize compounds for inhibition of TgCDPK1 enzymatic activity. The first series explored variation of the R<sub>2</sub> substructure in the context of a naphthylmethylene R<sub>1</sub>-bearing pyrazolopyrimidine core scaffold (substituent **10** in Figure 1). From that series, several piperidine-containing R<sub>2</sub> substructures were found that confer potent inhibition of TgCDPK1 enzymatic activity, the best being the 4-piperidinemethyl R<sub>2</sub> substructure of analogue **10n** (TgCDPK1 IC<sub>50</sub> = 15 nM). X-ray crystallographic analysis showed that the 4-piperidinemethyl group is oriented toward the αD-helix and makes a solvent exposed salt bridge with the Glu135 side chain carboxylate (as exemplified in the cocrystal structure of compound **15n** bound to TgCDPK1, presented in Figure 2B). The second series of inhibitors evaluated variation at the R<sub>1</sub> position and identified several groups that were superior to the naphthylmethylene substructure for conferring potent inhibition of TgCDPK1 activity. These contain R<sub>1</sub> aryl groups directly linked to the pyrazolopyrimidine core (i.e., through a C<sub>aryl</sub>-C<sub>aryl</sub> linkage), which orients the R<sub>1</sub> substructures toward the Gly128 gatekeeper residue and into an adjacent hydrophobic pocket (Figure 2). This increases selectivity for TgCDPK1 over potential off-target human kinases, which primarily contain threonine and larger gatekeeper residues that hinder access to this pocket.

On the basis of the structure–activity relationships generated in our previous study, we have designed, synthesized, and evaluated a subsequent panel of lead TgCDPK1 enzyme inhibitors for their ability to prevent the invasion of *T. gondii* parasites into host cells. In the first part of this study, we have investigated a panel of R<sub>1</sub> groups in the context of <sup>i</sup>Pr, <sup>t</sup>Bu, and 4-piperidinemethyl substituents at the R<sub>2</sub> position (series **a**, **b**, and **n** in Figure 1 and Table 1). To impart selective inhibition for TgCDPK1 over human kinases, our efforts focused on R<sub>1</sub> substructures that occupy the enlarged hydrophobic pocket next to the Gly128 gatekeeper residue, such as substituted phenyls, indoles, indazoles, naphthyls, and quinolines (Figure 1). From previous structural studies,<sup>15</sup> it appeared that increased binding affinity could be gained by extending the R<sub>1</sub> substructure more deeply into the adjacent hydrophobic pocket (Figure 2C). To explore this possibility, analogues with extended R<sub>1</sub> groups (series **14**–**25**) were synthesized. Analysis of various R<sub>2</sub> substructures in the context of multiple R<sub>1</sub> groups allows the interdependence of these two positions to be explored.

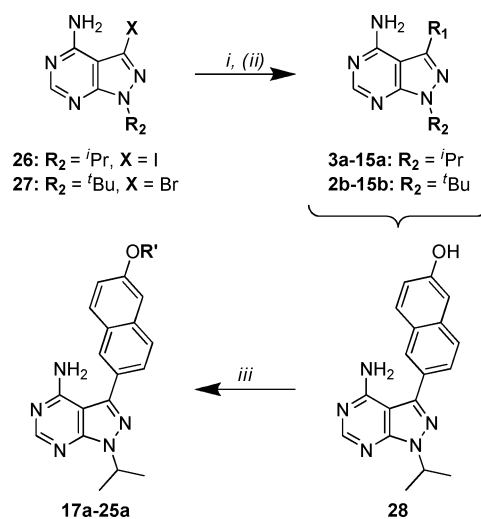
Syntheses of pyrazolopyrimidine compounds with <sup>i</sup>Pr or <sup>t</sup>Bu groups at the R<sub>2</sub> position (series **a** and **b**) are outlined in Scheme 1. Detailed procedures and characterization data for all compounds are presented in the Supporting Information. Microwave-assisted Suzuki–Miyaura reactions were employed for the coupling of R<sub>1</sub> boronic acids or boronate pinacol esters to the respective pyrazolopyrimidine halide intermediates **26** and **27**.<sup>16,17</sup> For compounds **17a**–**25a**, containing extended R<sub>1</sub> substructures, Suzuki–Miyaura coupling of the TBDMS-protected boronic acid conveniently afforded the deprotected naphthol intermediate directly, which was subsequently alkylated with the respective R' halide. Synthesis of the 4-piperidinemethylpyrazolopyrimidine compounds (series **n**) is outlined in Scheme 2. The pyrazolopyrimidine core scaffold intermediate **32** was synthesized according to previously reported procedures.<sup>16,17</sup> Pyrazolopyrimidine **32** was then alkylated with mesylate **30** to afford the key intermediate **34**. Suzuki–Miyaura coupling of the respective R<sub>1</sub> boronic acids or boronate pinacol esters and subsequent naphthol alkylations were performed as

**Table 1. Enzymatic Assay ( $IC_{50}$ ) and *T. gondii* Proliferation ( $EC_{50}$ ) Results for Compounds with Variable  $R_1$  Substructures (1–25) across the  $R_2$  Series a, b, and n<sup>a</sup>**

compd		kinase enzymatic $IC_{50}$ ( $\mu M$ )			<i>T. gondii</i> proliferation $EC_{50}$ ( $\mu M$ )
		<i>Tg</i> CDPK1	<i>Tg</i> CDPK1 (G128M)	SRC	
1	b	>5	>3	>10	>6.25
	n	>5	>3	>10	>6.25
2	b	0.0045	>3	0.13	0.23
	n	0.058	>3	>10	
3	a	0.019	>3	1.3	0.51
	b	0.0073	>3	0.58	0.041
4	a	0.040	>3	5.1	
5	a	0.0050	>3	0.65	0.080
	b	0.0041	>3	0.18	0.0030
	n	0.0022	>3	>10	1.7
6	a	0.012	>3	1.5	0.15
	n	0.081	>3	>10	
7	a	0.0091	>3	1.2	0.27
	n	0.018	>3	>10	>6.25
8	a	0.0036	>3	0.29	0.12
	b	0.013	>3	0.52	0.044
9	b	0.0025	>3	2.1	0.12
	n	0.0037	>3	>10	>6.25
10	a	0.13	>3	8.8	
	b	0.031	>3	2.2	
	n	0.015	>3	>10	2.2
11	a	0.0050	>3	0.065	0.072
	b	0.0079	>3	0.12	0.35
	n	0.0025	>3	>10	0.63
12	a	0.024	>3	0.20	0.52
	b	0.018	>3	>10	>6.25
13	b	0.0031	>3	4.1	0.11
	n	0.0054	>3	>10	>6.25
14	a	0.0060	>3	0.67	0.021
	b	0.020	>3	2.0	0.010
	n	0.0049	>3	>10	0.41
15	a	0.0050	>3	0.38	0.018
	b	0.033	>3	2.2	
	n	0.0025	>3	>10	0.052
16	n	0.0034	>3	>10	0.058
17	a	0.010	>3	0.55	0.33
	n	0.0038	>3	>10	0.50
18	a	0.0006	>3	0.20	0.010
	n	0.0030	>3	>10	0.12
19	a	0.0032	>3	0.30	>6.25
	n	0.0026	>3	>10	0.16
20	a	0.0054	>3	0.26	0.31
	b	0.20	>3	1.1	
	n	0.0037	>3	>10	0.21
21	a	0.0009	>3	0.78	0.090
	n	0.0037	>3	>10	0.060
22	a	0.0008	>3	0.041	0.0033
	n	0.0023	0.94	3.1	0.13
23	a	0.011	>3	0.28	0.14
	n	0.0013	>3	1.8	1.1
24	a	0.0055	>3	0.28	0.012
	n	0.0007	1.3	0.38	0.10
25	a	0.0040	>3	0.27	0.013
	n	0.0007	1.1	1.6	0.46

<sup>a</sup>All results are the averages of at least three assays. Heat map representation of  $IC_{50}$  and  $EC_{50}$  results are presented in Table 2.

**Scheme 1. General Synthetic Procedures for Compound Series a and b<sup>a</sup>**



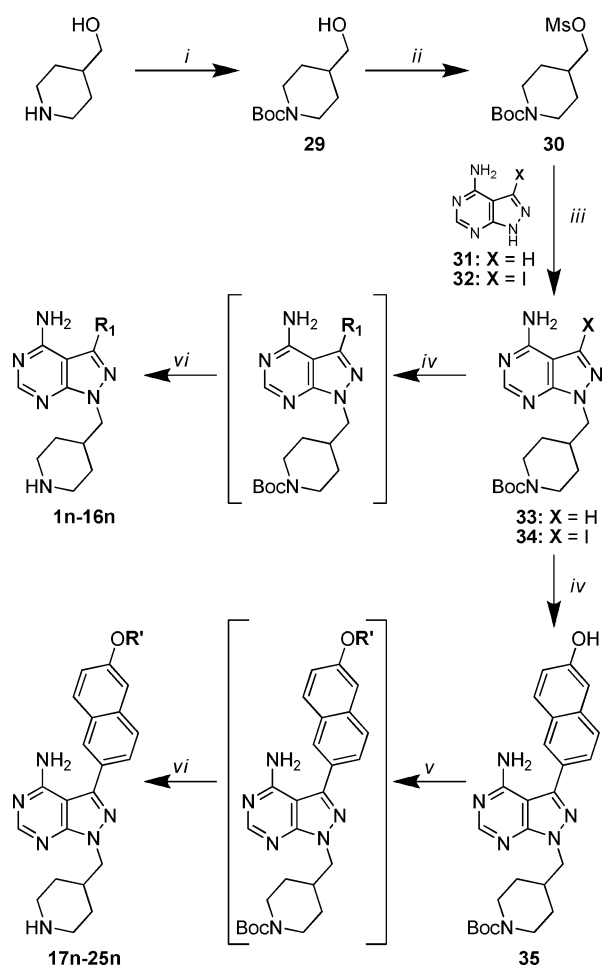
<sup>a</sup>(i)  $\text{Na}_2\text{CO}_3$ ,  $\text{Pd}(\text{PPh}_3)_4$ , boronic acid or boronate pinacol ester,  $\text{H}_2\text{O}/\text{DME}$ ,  $80^\circ\text{C}$ ; (ii)  $\text{TFA}/\text{CH}_2\text{Cl}_2$  (for Boc-protected  $R_1$  substructures 6 and 7); (iii)  $R'$  halide,  $\text{K}_2\text{CO}_3$ ,  $\text{DMF}$ , room temperature or  $80^\circ\text{C}$ .

described above for the series a and b compounds. Boc-containing compounds were deprotected using 50%  $\text{TFA}$  in  $\text{CH}_2\text{Cl}_2$  and converted to their  $\text{HCl}$  salts for enzymatic and cell-based evaluation (results are discussed below and presented in Tables 1 and 2).

From the compounds described in Table 1, the 6-ethoxynaphthyl  $R_1$  group (15) were identified as the best substructure for conferring potent inhibition of *Tg*CDPK1 enzymatic activity and *T. gondii* cell proliferation (vide infra). Therefore, a second series of compounds containing a 6-ethoxynaphthyl  $R_1$  and variable  $R_2$  substructures was generated (Figure 1, substructures a–w). Syntheses of these compounds are presented in Scheme 3. For the piperidinylamide and sulfonamide compounds (15l, 15m, 15q, and 15r), the pyrazolopyrimidine intermediate core 32 was alkylated with mesylates 36, 37, 40, and 41, respectively, followed by microwave-assisted Suzuki–Miyaura coupling with 6-ethoxynaphthyl-2-boronic acid as described above (Scheme 3A). Compounds 15o and 15p were synthesized by reductive alkylation of 15n with formaldehyde and acetaldehyde, respectively, using sodium cyanoborohydride (Scheme 3B). The remaining series 15 compounds were synthesized by first appending the 6-ethoxynaphthyl  $R_1$  substructure to the pyrazolopyrimidine core scaffold 32 through microwave-assisted Suzuki–Miyaura couplings, affording intermediate 44. Mitsunobu alkylation of the remaining  $R_2$  groups using resin-bound  $\text{PPh}_3$ , followed by Boc-deprotection with  $\text{TFA}/\text{CH}_2\text{Cl}_2$ , afforded compounds 15c, 15e, 15g, and 15s. Reductive alkylation of the deprotected intermediates, with respective  $R_2$  aldehydes, provided final compounds 15d, 15f, 15h–k, and 15t–w (compounds 15k and 15w required additional Boc-deprotection). All compounds were purified by preparatory RP-HPLC, and amine-containing compounds were converted to their  $\text{HCl}$  salts for enzymatic and cell-based evaluation (results are discussed below).

**Pyrazolopyrimidines Are Potent Inhibitors of *Tg*CDPK1 Enzymatic Activity.** Compounds were first evaluated for their ability to inhibit the in vitro enzymatic activity of wild type *T. gondii* CDPK1. Inhibition was determined



Scheme 2. General Synthetic Procedures for Compound Series n<sup>a</sup>

<sup>a</sup>(i)  $\text{Boc}_2\text{O}$ ,  $\text{CH}_2\text{Cl}_2$ ; (ii) methanesulfonyl chloride, TEA,  $\text{CH}_2\text{Cl}_2$ , 0 °C to room temperature; (iii)  $\text{Cs}_2\text{CO}_3$ , DMF, room temperature or 80 °C; (iv)  $\text{Na}_2\text{CO}_3$ ,  $\text{Pd}(\text{PPh}_3)_4$ , boronic acid or boronate pinacol ester,  $\text{H}_2\text{O}/\text{DME}$ , 80 °C; (v) R' halide,  $\text{K}_2\text{CO}_3$ , DMF, room temperature or 80 °C; (vi) TFA/ $\text{CH}_2\text{Cl}_2$ .

using a previously reported luminescence-based kinase assay.<sup>16</sup> Although a large percentage of the compounds tested displayed very potent inhibition of *Tg*CDPK1, several notable trends were observed. While the absence of a hydrophobic substituent at the R<sub>1</sub> position renders these pyrazolopyrimidine compounds inactive against *Tg*CDPK1 (the IC<sub>50</sub> values for **1b** and **1n** are >5 μM, Table 1), incorporation of R<sub>1</sub> substructures as small as a phenyl group confers potent enzymatic inhibition. Overall, 86% of the compounds tested have IC<sub>50</sub> < 25 nM against *Tg*CDPK1 (Table 1). When compared with results obtained in our previous study,<sup>16</sup> it is evident that coupling of an R<sub>1</sub> substructure to the pyrazolopyrimidine core through a direct C<sub>aryl</sub>–C<sub>aryl</sub> linkage provides analogues with superior potency relative to those that contain a methylene spacer (for example, series **10**). As observed from crystallographic studies, this direct linkage orients the R<sub>1</sub> substructures toward the adjacent pocket next to the Gly128 gatekeeper residue, allowing large hydrophobic groups to make extensive contacts (Figure 2).<sup>18</sup> In the context of the 6-ethoxynaphthyl R<sub>1</sub> substructure (series **15**), it appears that a wide variety of substitutions at the R<sub>2</sub> position are well tolerated for maintaining potent *Tg*CDPK1 enzymatic inhibition (Table 3), which is in

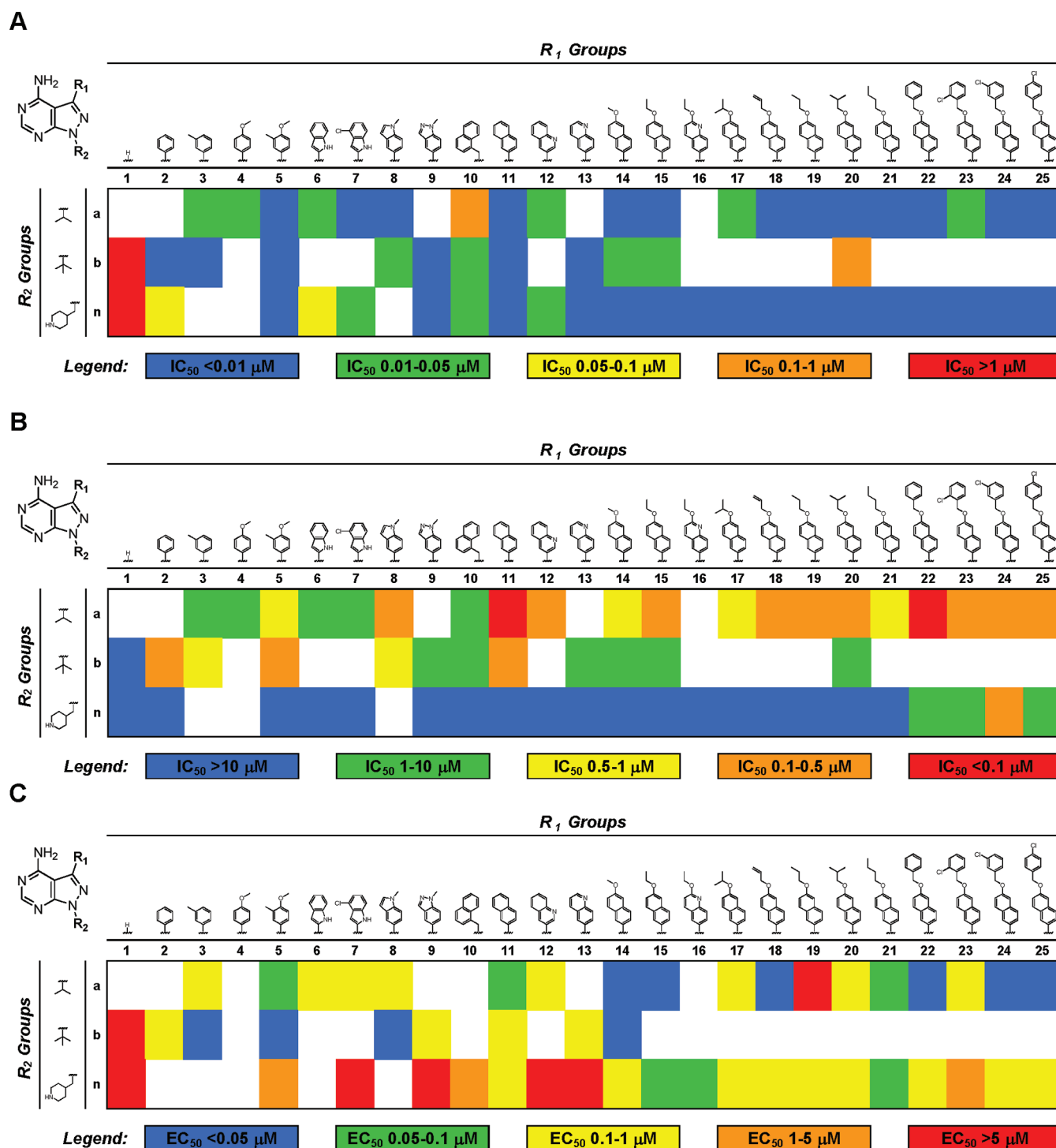
contrast to analogues that contain a naphthylmethylene group at this position. For example, series **15** compounds (6-ethoxynaphthyl R<sub>1</sub>) that are alkylated, acetylated, or sulfonylated on the piperidine rings of their R<sub>2</sub> substructures maintain low nanomolar inhibition of *Tg*CDPK1 enzymatic activity, whereas series **10** analogues (naphthylmethylene R<sub>1</sub>) containing similar modifications demonstrate IC<sub>50</sub> values in the high nanomolar range. Consistently potent inhibition across a wide range of R<sub>1</sub> and R<sub>2</sub> substructures suggests there is ample chemical space at either position to exploit for optimizing the pharmacological properties of these inhibitors.

To determine how a larger gatekeeper residue affects compound binding, inhibitors were tested against a *Tg*CDPK1 mutant enzyme that contains methionine at this position (Gly128Met). Molecular modeling predicts that the increased steric bulk of this residue should clash with large R<sub>1</sub> substructures (Figure 2B). In addition, the Gly128Met mutant was selected as a drug-resistant mutant because it maintains enzymatic activity comparable to that of wild type *Tg*CDPK1 and is able to complement for loss of endogenous enzyme activity in *T. gondii* parasites. In nearly all cases, the presence of the larger methionine side chain abolishes the inhibitory activity of these molecules (IC<sub>50</sub> values are generally >3 μM). Even for compounds **22n**, **24n**, **25n**, **15h**, **15k**, and **15s–w**, which show some activity against Gly128Met *Tg*CDPK1, the differences in IC<sub>50</sub> values between the wild type and mutant enzymes are >250-fold (with the exception of **15w**, which displays a 68-fold difference). Thus, the presence of a small gatekeeper residue provides a distinct preference for binding to the wild type enzyme. These results are promising for the development of pyrazolopyrimidine inhibitors as potential antiparasitic drugs because it suggests we should be able to obtain selectivity for *Tg*CDPK1 over human kinases, which do not contain gatekeeper residues as small as Gly or Ala.

**Lead Compounds Selectively Inhibit *Tg*CDPK1 over Human Kinases and Do Not Inhibit Growth of Human Cell Lines.** While compound evaluation in the Gly128Met *Tg*CDPK1 enzymatic assay was an important surrogate for gauging potential inhibition of off-target kinases that contain larger gatekeeper residues in an otherwise identical binding site, further evaluation was performed against a panel of human kinases. Compounds were first tested against SRC kinase, as prior selectivity studies have demonstrated that similar pyrazolopyrimidine-based inhibitors preferentially target this enzyme.<sup>19–21</sup> Since SRC contains a threonine gatekeeper residue, which is one of the smallest amino acid side chains present at this position in human kinases, we selected this enzyme as a surrogate for probing potential off-target kinase activity. Inhibition of this enzyme serves as a first-pass filter to prioritize lead candidates for subsequent cell-based evaluation. Inhibition values were determined using a previously reported radioactive kinase assay.<sup>16</sup>

The activities of the first series of compounds against SRC are shown in Table 1. While we had initially envisioned the R<sub>1</sub> substructure providing the primary determinant for obtaining selective inhibition of *Tg*CDPK1 over human kinases (i.e., a steric clash of the R<sub>1</sub> substructures with the larger gatekeeper residue side chains obstructs ligand binding), this appears to be only partially true. For 93% of the compounds tested, IC<sub>50</sub> values are at least 25-fold higher for SRC than for *Tg*CDPK1 (Table 1). Thus, substitution at the R<sub>1</sub> substructure is a significant determinant of selective inhibition of *Tg*CDPK1. However, further examination of the results presented in Table 1,

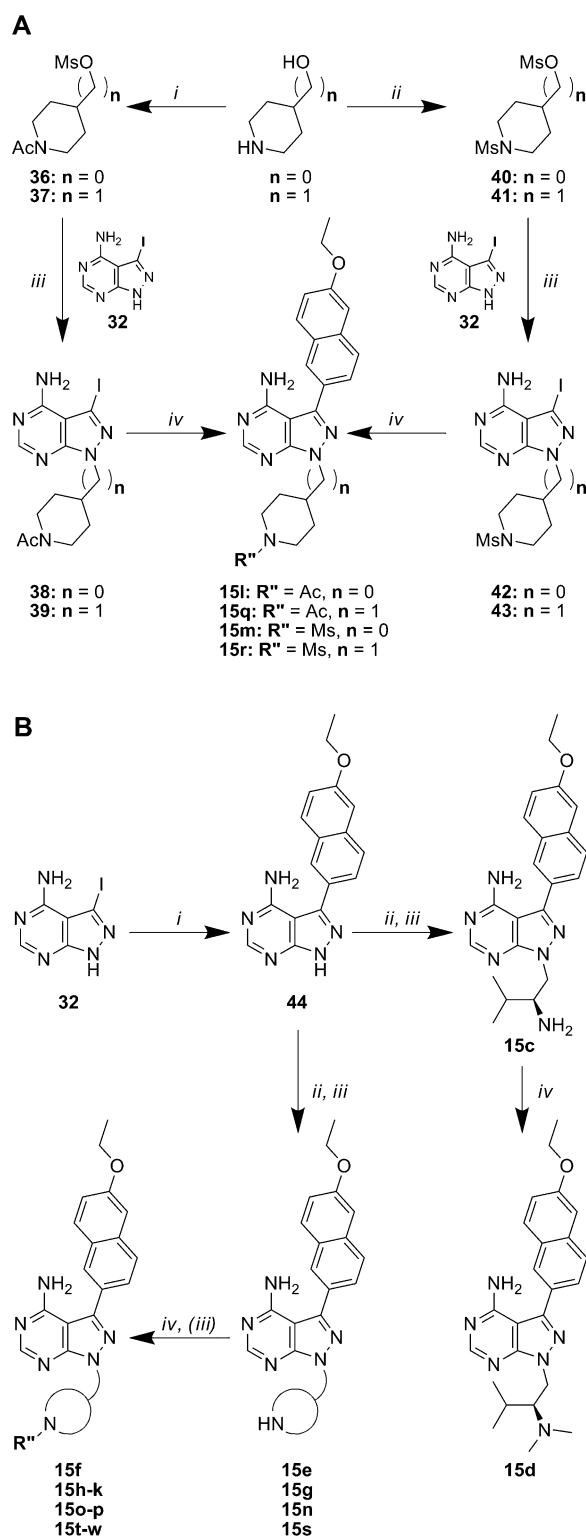
Table 2. Heat Map Representation of (A) Wild Type *Tg*CDPK1 Enzymatic  $IC_{50}$  from Table 1, (B) SRC Enzymatic  $IC_{50}$  from Table 1, and (C) Wild Type *T. gondii* Proliferation  $EC_{50}$  from Table 1<sup>a</sup>



<sup>a</sup>Blue represents compounds with desirable  $IC_{50}$  or  $EC_{50}$  values, transitioning to red for compounds with undesirable activities.

where we have evaluated  $R_1$  substructures in the context of <sup>t</sup>Pr (a), <sup>t</sup>Bu (b), and 4-piperidinomethyl (n)  $R_2$  substituents, demonstrates a striking trend where the <sup>t</sup>Pr- and <sup>t</sup>Bu-containing compounds are consistently less selective for *Tg*CDPK1 over SRC than the 4-piperidinomethyl analogues (differences are readily observed in the inhibition heat maps in parts A and B of Table 2 and Figure S1 in the Supporting Information). The second compound series, where we have evaluated  $R_2$  substructures in the context of a 6-ethoxynaphthyl (15)

group at the  $R_1$  position, was tested against SRC to further probe this interesting phenomenon (Table 3). In this series, it appears that compounds that contain a methylene spacer adjacent to the pyrazolopyrimidine core display greater selectivity for *Tg*CDPK1 inhibition over SRC. 4-Piperidinomethyl-containing compounds (n-r) are particularly selective and display no inhibition of SRC activity at compound concentrations upward of  $10 \mu M$ . Thus, it is evident that the degree of selective inhibition of *Tg*CDPK1 over SRC results

Scheme 3. General Synthetic Procedures for Compound Series 15<sup>a</sup>

<sup>a</sup>(A) (i)  $\text{Ac}_2\text{O}$ , TEA,  $\text{CH}_2\text{Cl}_2$ , then methanesulfonyl chloride; (ii) methanesulfonyl chloride, TEA,  $\text{CH}_2\text{Cl}_2$ ; (iii)  $\text{Cs}_2\text{CO}_3$ , DMF,  $80^\circ\text{C}$ ; (iv)  $\text{Na}_2\text{CO}_3$ ,  $\text{Pd}(\text{PPh}_3)_4$ , boronic acid or boronate pinacol ester,  $\text{H}_2\text{O}/\text{DME}$ ,  $80^\circ\text{C}$  in microwave. (B) (i)  $\text{Na}_2\text{CO}_3$ ,  $\text{Pd}(\text{PPh}_3)_4$ , 6-ethoxynaphthalene-2-boronic acid,  $\text{H}_2\text{O}/\text{DME}$ ,  $110^\circ\text{C}$ ; (ii) Boc- $R_2$ -OH, PS- $\text{PPh}_3$ , DIAD, THF, room temperature to  $70^\circ\text{C}$ ; (iii) TFA/ $\text{CH}_2\text{Cl}_2$ ; (iv) sodium methoxide in MeOH, then 2% AcOH,  $R''$ -aldehyde,  $\text{NaBH}_3\text{CN}$ .

Table 3. Enzymatic Assay ( $\text{IC}_{50}$ ) and *T. gondii* Proliferation ( $\text{EC}_{50}$ ) Results for Compounds with Variable  $R_2$  (a–w) Substructures and a 6-Ethoxynaphthyl Group (Series 15) at the  $R_1$  Position<sup>a</sup>

compd	kinase enzymatic $\text{IC}_{50}$ ( $\mu\text{M}$ )			<i>T. gondii</i> proliferation $\text{EC}_{50}$ ( $\mu\text{M}$ )
	<i>Tg</i> CDPK1	<i>Tg</i> CDPK1 (G128M)	SRC	
15-				
a	0.0050	>3	0.37	0.018
b	0.033	>3	2.2	
c	0.013	>3	>10	1.0
d	0.012	>3	>10	0.96
e	0.0091	>3	>10	0.97
f	0.0081	>3	>10	0.86
g	0.0026	>3	5.0	0.045
h	0.0024	2.6	5.6	0.050
i	0.0034	>3	8.7	0.090
j	0.0043	>3	>10	0.16
k	0.0043	0.98	0.73	0.34
l	0.0061	>3	1.6	0.029
m	0.0028	>3	0.81	0.035
n	0.0025	>3	>10	0.052
o	0.0029	>3	>10	0.14
p	0.0050	>3	>10	0.33
q	0.011	>3	>10	0.20
r	0.032	>3	>10	
s	0.0019	1.5	3.3	0.14
t	0.0022	1.4	5.2	0.049
u	0.0027	2.0	6.3	0.10
v	0.0030	2.9	6.7	0.18
w	0.0043	0.27	8.2	1.2

<sup>a</sup>All results are the averages of at least three assays.

from a synergy between the  $R_1$  and  $R_2$  substructures. A more detailed discussion of the structural underpinnings for this synergy will be presented in a forthcoming X-ray crystallography manuscript.<sup>18</sup>

Several lead compounds (14a, 14n, 15a, 15h, 15n, 15o, and 16n) were further evaluated in an expanded panel of human kinases that all contain threonine gatekeeper residues (ABL, LCK, p38 $\alpha$ , EPHA3, CSK, and EGFR). In general, similar inhibition trends were observed for ABL, p38 $\alpha$ , EPHA3, CSK, and EGFR as described above (Table 4). In comparison to SRC, compounds generally display increased inhibition of LCK, equipotency against ABL and EGFR, and decreased inhibition of p38 $\alpha$ , EPHA3, and CSK, which is similar to trends that have been previously reported.<sup>19</sup> Importantly, we generally observe >1000-fold differences between  $\text{IC}_{50}$  values for *Tg*CDPK1 over human kinases for our lead inhibitors (14n, 15h, 15n, 15o, and 16n); refer to Table S1 in the Supporting Information for specific selectivity ratios between the human kinase  $\text{IC}_{50}$  values compared to *Tg*CDPK1). While these compounds have only been tested against a small panel of enzymes that were envisioned to be of primary concern for inhibition, these results suggest that our lead candidate *T. gondii* therapeutics should interact minimally with potential off-target human kinases.

As an indicator for potential host cell toxicity during toxoplasmosis therapy, we further evaluated our panel of *Tg*CDPK1 inhibitors (14a, 14n, 15a, 15h, 15n, 15o, and 16n) for their ability to inhibit the growth of human neutrophil (HL-60) and lymphocyte (CRL-8155) cell lines. Assays were performed with a similar procedure as previously reported.<sup>16</sup> These compounds

**Table 4. Enzymatic Assay Results (IC<sub>50</sub>) for an Expanded Panel of Human Kinases and Growth Inhibition (GI<sub>50</sub>) of Human Cell Lines<sup>a</sup>**

compd	kinase enzymatic IC <sub>50</sub> (μM)								human cells, GI <sub>50</sub> (μM)	
	TgCDPK1	SRC	ABL	LCK	p38α	EPHA3	CSK	EGFR	HL-60	CRL-8155
14a	0.0060	0.67	0.82	0.079	>10	1.6	2.6	0.51	>10	>10
14n	0.0049	>10	>10	0.62	>10	>10	>10	>10	>10	>10
15a	0.0050	0.38	1.7	0.052	>10	3.7	3.1	0.70	>10	>10
15h	0.0024	5.6	>10	0.12	>10	>10	10	>10	>10	>10
15n	0.0025	>10	>10	0.96	>10	>10	10	>10	>10	>10
15o	0.0029	>10	4.6	3.3	>10	>10	>10	>10	>10	>10
16n	0.0034	>10	>10	>10	>10	>10	>10	>10	>10	>10

<sup>a</sup>All results are the averages of at least three assays.

exhibited no inhibition of cell growth at concentrations up to 10 μM (Table 4). To better define potential therapeutic windows for our toxoplasmosis drug candidates, we are performing growth inhibition studies using higher compound concentrations and identifying drug levels required to clear parasitic infection in mammalian challenge models. Results from these studies will be presented elsewhere.

**Potent TgCDPK1 Enzymatic Inhibitors Block the Proliferation of *T. gondii* Parasites.** Having developed compounds that selectively inhibit TgCDPK1 over a panel of human kinases and do not inhibit the growth of human cell lines, we further investigated the most potent TgCDPK1 enzymatic inhibitors (IC<sub>50</sub> < 25 nM) for their efficacy in blocking the invasion of *T. gondii* parasites into human foreskin fibroblast cells. Since *T. gondii* is an obligate intracellular parasite, inhibition of host cell invasion blocks parasite replication, which was measured as a surrogate according to a slightly modified version of a previously reported procedure.<sup>15</sup> In these cellular assays, several prominent trends were observed. Notably, compounds **1b** and **1n**, which do not contain an R<sub>1</sub> substituent and are inactive against TgCDPK1 enzymatic activity, do not block *T. gondii* cell invasion/proliferation. Of the compounds that do potently inhibit TgCDPK1 enzymatic activity (IC<sub>50</sub> < 25 nM), an impressive 84% also effectively block *T. gondii* cell invasion/proliferation (EC<sub>50</sub> < 1 μM). Importantly, no inhibitor toxicity was observed against the human foreskin fibroblasts used in this assay. Thus, it seems unlikely that the decreased parasite growth is an artifact of host cell inhibition. Many of the 4-piperidinemethyl compounds are potent inhibitors of *T. gondii* proliferation. In particular, compounds bearing the 6-ethoxynaphthyl R<sub>1</sub> substructure (series **15**) are potent enzymatic and cell proliferation inhibitors across nearly the entire R<sub>2</sub> substructure panel. However, compounds containing an <sup>i</sup>Pr or <sup>t</sup>Bu group at the R<sub>2</sub> position (series **a** and **b**, respectively) are generally more potent inhibitors in the cell proliferation assay than their 4-piperidinemethyl analogues (series **n**). This is readily observed in Figure 3A and in the inhibition heat map presented in Table 2C. The **a** and **b** series of inhibitors are significantly more hydrophobic than the 4-piperidinemethyl-containing compounds (the piperidine amine would be protonated under physiological conditions), which may increase their membrane permeability. In addition, the greater potential of pyrazolopyrimidine inhibitors with <sup>i</sup>Pr and <sup>t</sup>Bu substituents at the R<sub>2</sub> position to inhibit off-target mammalian and parasitic kinases (as suggested by their more potent inhibition of SRC and other human kinases) may lead to enhanced cellular activity. While it is interesting to speculate on the biophysical underpinnings of these differences, SAR rationalizations in

these cellular assays are likely to be complicated and beyond the scope of this manuscript.

Three compounds (**15n**, **15o**, and **16n**) were evaluated in cell-based experiments using *T. gondii* parasites expressing the Gly128Met TgCDPK1 gatekeeper mutant, to further validate that TgCDPK1 is the primary target for the observed antiparasitic activity. The Gly128Met TgCDPK1 variant is functionally active and complements the loss of endogenous wild type enzyme activity, permitting parasite invasion and proliferation in host cells. For all three compounds, a significant increase in *T. gondii* proliferation EC<sub>50</sub> (8- to 26-fold) was observed for parasites expressing the Gly128Met TgCDPK1 mutant over those expressing wild type TgCDPK1 at similar levels or nontransfected parasites (Figure 3B and Figure S2 in the Supporting Information). The observed inhibitory effects at higher compound concentrations (EC<sub>50</sub> ≈ 1–3 μM for the Gly128Met TgCDPK1 expressing parasites) could indicate off-target inhibition of another parasite kinase. However, the dramatic EC<sub>50</sub> shifts seen for all three inhibitors demonstrate that TgCDPK1 is the primary target for blocking parasite invasion and proliferation.

## CONCLUSIONS

In the present study, we have evaluated over 70 ATP-competitive inhibitors of TgCDPK1 for their utility as potential toxoplasmosis therapeutics. We found that inhibition of TgCDPK1 enzymatic activity correlates strongly with inhibition of *T. gondii* proliferation. Of the 64 compounds that are potent inhibitors of TgCDPK1 enzymatic activity in vitro (IC<sub>50</sub> < 25 nM), 83% exhibit EC<sub>50</sub> < 1 μM in a parasite invasion/proliferation assay. Furthermore, 38% exhibit EC<sub>50</sub> < 100 nM. In a rescue experiment, expression of the drug-resistant Gly128Met TgCDPK1 enzyme in parasites verified that inhibition of endogenous wild type CDPK1 is the primary mechanism of action for these compounds. By virtue of the small glycine gatekeeper residue in wild type TgCDPK1, these “bumped” kinase inhibitors are able to selectively inhibit the parasite enzyme over human kinases, which contain gatekeeper residues larger than glycine that sterically hinder inhibitor binding. This selectivity is mimicked in cellular assays where compounds potently inhibit *T. gondii* proliferation but do not affect the growth of human cell lines. Compounds exhibiting large therapeutic windows between inhibition of *T. gondii* proliferation and human cell growth (e.g., >100–1000×) are undergoing additional preclinical drug development testing to evaluate pharmacological properties such as solubility, pharmacokinetics, pharmacodynamics, and metabolism. The results obtained here poise us for future studies to evaluate lead candidates possessing favorable properties in parasitic challenge models in mice as a therapeutic proof of principle.



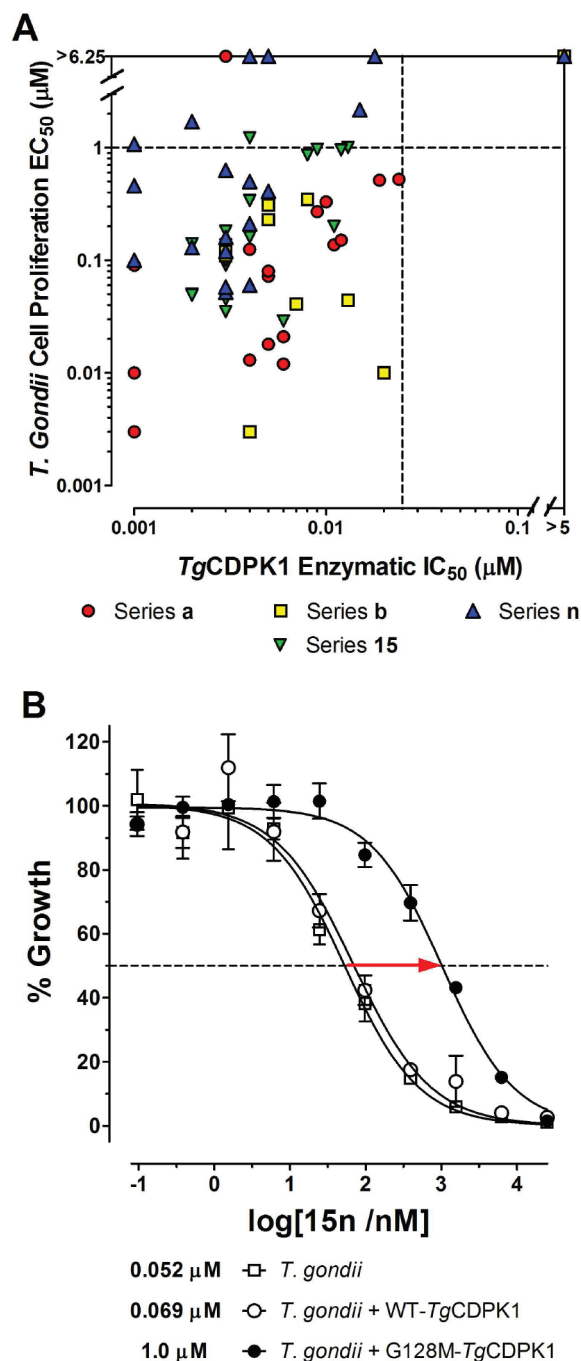


**Figure 3.** Enzymatic and cellular inhibition of *TgCDPK1*. (A) Correlation between *T. gondii* cell proliferation  $EC_{50}$  and *TgCDPK1* enzymatic  $IC_{50}$  results. The solid lines at  $EC_{50} > 6.25 \mu\text{M}$  and  $IC_{50} > 5 \mu\text{M}$  represent the upper detection limits for compounds tested in the respective assays. Of the 62 compounds displaying *TgCDPK1* enzymatic  $IC_{50} < 0.025 \mu\text{M}$ , 86% are also potent inhibitors of *T. gondii* invasion/proliferation ( $EC_{50} < 1 \mu\text{M}$ , points in bottom left quadrant). (B) Comparison of  $EC_{50}$  curves between wild type *T. gondii* (open squares) and parasites expressing either wild type *TgCDPK1* (open circles) or the drug resistant Gly128Met *TgCDPK1* mutant (closed circles). Expression of the drug resistant Gly128Met *TgCDPK1* mutant rescues cells from the potent antiproliferative effects of inhibitor 15n.

## EXPERIMENTAL PROCEDURES

**General Synthetic Methods.** Unless otherwise stated, all chemicals were purchased from commercial suppliers and used

without further purification. Reaction progress was monitored by thin-layer chromatography on silica gel 60 F254 coated glass plates (EM Sciences). Chromatography was performed using an IntelliFlash 280 automated flash chromatography system, eluting on prepacked Varian SuperFlash silica gel columns with hexanes/EtOAc or  $\text{CH}_2\text{Cl}_2/\text{MeOH}$  gradient solvent systems. For preparative HPLC purification, samples were chromatographically separated using a Varian Dynamax Microsorb 100-5  $\text{C}_{18}$  column (250 mm  $\times$  21.4 mm), eluting with  $\text{H}_2\text{O}/\text{CH}_3\text{CN}$  or  $\text{H}_2\text{O}/\text{MeOH}$  gradient solvent systems (+0.05% TFA). The purity of all final compounds was determined by two analytical RP-HPLC methods, using an Agilent ZORBAX SB- $\text{C}_{18}$  (2.1 mm  $\times$  150 mm) or Varian Microsorb-MV 100-5  $\text{C}_{18}$  column (4.6 mm  $\times$  150 mm) and eluting with either  $\text{H}_2\text{O}/\text{CH}_3\text{CN}$  or  $\text{H}_2\text{O}/\text{MeOH}$  gradient solvent systems (+0.05% TFA) run over 30 min. Products were detected by UV at  $\lambda = 254 \text{ nm}$ , with all final compounds displaying  $>95\%$  purity. NMR spectra were recorded on Bruker 300 or 500 MHz spectrometers at ambient temperature. Chemical shifts are reported in parts per million ( $\delta$ ) and coupling constants in Hz.  $^1\text{H}$  NMR spectra were referenced to the residual solvent peaks as internal standards (7.26 ppm for  $\text{CDCl}_3$ , 2.50 ppm for  $\text{DMSO}-d_6$ , and 3.34 ppm for  $\text{CD}_3\text{OD}$ ). Mass spectra were recorded with a Bruker Esquire liquid chromatograph-ion trap mass spectrometer. Inhibitors were synthesized through several different routes, as represented in Schemes 1–3. Syntheses of compounds 1b, 3a, 4a, 5a, 10a, 10b, 10n, 11a, 11b, 12a, 14a, 15a, 26, 27, 31, and 32 have been previously reported.<sup>16,17</sup> All other synthesis and compound characterization data are presented in the Supporting Information.

***T. gondii* CDPK1 Enzymatic Assays.** Expression, purification, and enzymatic evaluation of wild type and Gly128Met gatekeeper mutant *TgCDPK1* were performed as described previously.<sup>15,16</sup> Briefly, enzymatic reactions were performed with 4 nM of either wild type or Gly128Met *TgCDPK1* in assay buffer containing 20 mM HEPES (pH 7.5), 0.1% BSA, 10 mM  $\text{MgCl}_2$ , 1 mM EGTA, 2 mM  $\text{CaCl}_2$ , 10  $\mu\text{M}$  ATP, and 40  $\mu\text{M}$  syntide-2 peptide substrate (peptide sequence: PLARTLSVAGLPGKK-OH). After incubation for 90 min at 30  $^\circ\text{C}$ , the enzymatic reactions were terminated by adding EGTA to a final concentration of 5 mM. The amount of ATP remaining in solution was evaluated using the Kinase Glo luciferase assay from Promega, with sample luminescence read using a Microbeta 2 plate reader (Perkin-Elmer, Waltham, MA). Results were converted to percent inhibition, and  $IC_{50}$  values were calculated using nonlinear regression analysis in GraphPad Prism. Compounds were evaluated in triplicate in eight-point dilutions (3-fold dilution series) during the enzymatic reactions.

**Human Kinase Enzymatic Assays.** All compounds were evaluated in a primary counterscreen against SRC kinase using either the truncated catalytic kinase domain (SRCKD) or the three domain enzyme (SRC3D). Results from compounds tested with both KD and 3D enzymes demonstrated no significant difference in  $IC_{50}$  values and are thus reported together simply as inhibition of “SRC” kinase. Lead compounds were further evaluated against a small panel of additional human kinases: ABL, LCK, p38 $\alpha$ , EPHA3, CSK, and EGFR. Compounds were evaluated in 10-point, 3-fold dilution series ranging from 10  $\mu\text{M}$  to 0.5 nM during the enzymatic reactions, as per previously reported procedures.<sup>16</sup> Results were converted to percent inhibition, and  $IC_{50}$  values were calculated using nonlinear regression analysis in GraphPad Prism. Experiments were performed in triplicate or quadruplicate. Assay buffers, enzyme concentrations, substrate peptide sequences and concentrations, and enzymatic reaction times are listed in the assay-specific details presented below. All assays were performed using  $<5 \mu\text{M}$  ATP ( $[\text{ATP}] \ll K_m$ ).

- (1) SRC. Kinase concentration during the enzymatic reaction: 1 nM for SRCKD or 2 nM for SRC3D. Assay buffer: 33.5 mM HEPES, pH 7.5, 6.7 mM  $\text{MgCl}_2$ , 1.7 mM EGTA, 67 mM NaCl, 2 mM  $\text{Na}_3\text{VO}_4$ , 0.08 mg/mL BSA,  $\gamma^{32}\text{P}$  ATP (0.2  $\mu\text{Ci}/\text{well}$ ). Enzymatic reaction time: 30 min for SRCKD or 60 min for SRC3D. Substrate peptide sequence and concentration: Ac-EIYGEFKKK-OH (100  $\mu\text{M}$ ).
- (2) ABL. Kinase concentration during the enzymatic reaction: 1 nM for ABLKD or 2 nM for ABL3D. Assay buffer: 33.5 mM

- HEPES, pH 7.5, 6.7 mM MgCl<sub>2</sub>, 1.7 mM EGTA, 67 mM NaCl, 2 mM Na<sub>3</sub>VO<sub>4</sub>, 0.08 mg/mL BSA,  $\gamma^{32}\text{P}$  ATP (0.2  $\mu\text{Ci}/\text{well}$ ). Enzymatic reaction time: 30 min for ABLKD and 60 min for ABL3D. Substrate peptide sequence and concentration: Ac-EAIYAAPFAKKK-OH (100  $\mu\text{M}$ ).
- (3) LCK. Kinase concentration during the enzymatic reaction: 10 nM. Assay buffer: 75 mM HEPES, pH 7.5, 15 mM MgCl<sub>2</sub>, 3.75 mM EGTA, 150 mM NaCl, 2 mM Na<sub>3</sub>VO<sub>4</sub>, 0.08 mg/mL BSA,  $\gamma^{32}\text{P}$  ATP (0.2  $\mu\text{Ci}/\text{well}$ ). Enzymatic reaction time: 60 min. Substrate peptide sequence and concentration: Ac-EIYGEFKKK-OH (100  $\mu\text{M}$ ).
- (4) p38 $\alpha$ . Kinase concentration during the enzymatic reaction: 2 nM. Assay buffer: 75 mM HEPES, pH 7.5, 15 mM MgCl<sub>2</sub>, 3.75 mM EGTA, 150 mM NaCl, 2 mM Na<sub>3</sub>VO<sub>4</sub>, 0.08 mg/mL BSA, 1.9 mM BME,  $\gamma^{32}\text{P}$  ATP (0.2  $\mu\text{Ci}/\text{well}$ ). Enzymatic reaction time: 180 min. Substrate peptide and concentration: myelin basic protein (0.2 mg/mL).
- (5) EPHA3. Kinase concentration during the enzymatic reaction: 10 nM. Assay buffer: 30 mM HEPES, pH 7.5, 38 mM MgCl<sub>2</sub>, 630  $\mu\text{M}$  EGTA, 2 mM Na<sub>3</sub>VO<sub>4</sub>, 40  $\mu\text{g}/\text{mL}$  BSA,  $\gamma^{32}\text{P}$  ATP (0.2  $\mu\text{Ci}/\text{well}$ ). Enzymatic reaction time: 120 min. Substrate peptide and concentration: myelin basic protein (0.2 mg/mL).
- (6) CSK. Kinase concentration during the enzymatic reaction: 5 nM. Assay buffer: 75 mM HEPES, pH 7.5, 15 mM MgCl<sub>2</sub>, 3.75 mM EGTA, 150 mM NaCl, 2 mM Na<sub>3</sub>VO<sub>4</sub>, 0.2 mg/mL BSA,  $\gamma^{32}\text{P}$  ATP (0.2  $\mu\text{Ci}/\text{well}$ ). Enzymatic reaction time: 180 min. Substrate peptide sequence and concentration: Ac-KKKKEIYFFF-OH (130  $\mu\text{M}$ ).
- (7) EGFR. Kinase concentration during the enzymatic reaction: 1 nM. Assay buffer: 37.5 mM Tris, pH 7.5, 15 mM MgCl<sub>2</sub>, 0.75 mM EGTA, 0.75 mM Na<sub>3</sub>VO<sub>4</sub>, 0.015% Triton X-100, 3.75 mM DTT, 0.08 mg/mL BSA, 2 mM ATP,  $\gamma^{32}\text{P}$  ATP (0.2  $\mu\text{Ci}/\text{well}$ ). Enzymatic reaction time: 30 min. Substrate peptide and concentration: poly Glu-Tyr substrate (0.2 mg/mL).

**Human Cell Growth Inhibition Assays.** Lead compounds were evaluated for potential toxicity against two human cell lines: HL-60 (neutrophil) and CRL-8155 (lymphocytic) cells. Cells were grown in either IMDM (HL-60) or RPMI-1640 (CRL-8155) growth medium supplemented with 10% heat inactivated fetal calf serum and 2 mM L-glutamine. HL-60 growth medium additionally contained 25 mM HEPES and 1% penicillin/streptomycin. CRL-8155 growth medium additionally contained 10 mM HEPES, 1 mM sodium pyruvate, 4.5 g/L glucose, and 1.5 g/L sodium bicarbonate. Cells were grown in the presence of 10  $\mu\text{M}$  test compound for 48 or 72 h at 37 °C and 5% CO<sub>2</sub> in 96-well flat-bottom plates (Corning). Growth was quantified using Alamar blue as a developing reagent and detecting sample absorbance at  $\lambda = 570$  nm (600 nm reference wavelength). Percent growth inhibition by test compounds were calculated based on cultures incubated with DMSO negative and tipifarnib (R115777) positive controls (0% and 100% growth inhibition, respectively). All assays were performed in triplicate.

***T. gondii* Cell Proliferation Assays.** The invasion assay was performed as previously described,<sup>15</sup> with slight modifications to improve assay sensitivity and reliability. Compounds were diluted in DMEM maintaining 0.5% DMSO. *T. gondii* clonal parasites (10<sup>3</sup>) expressing  $\beta$ -galactosidase as a reporter (genotype RH $\Delta$ hxgprt,  $\beta$ -galactosidase, GFP<sup>15</sup> for the standard protocol) were mixed with the medium containing the compounds (200  $\mu\text{L}$ ) and incubated at 37 °C, 5% CO<sub>2</sub> for ~5 min. The parasite/compound mixture was added to 96-well plates containing confluent human fibroblast cell layers (from which growth medium was aspirated) and incubated for 44 h at 37 °C and 5% CO<sub>2</sub>. As a control, a dilution series of *T. gondii* (10<sup>3</sup>-0) parasites was grown in the same conditions described above but without compound. Plates were visually inspected for evidence of cytotoxic effects on fibroblasts.  $\beta$ -Galactosidase was then assayed using chlorophenol red  $\beta$ -galactopyranose (Sigma) as a substrate.<sup>22</sup> Plates were developed for ~1.5 h at 37 °C. Absorbance was measured at 595 nm on a SpectraMax M2 (Molecular Devices) microplate reader. Each experiment was performed in triplicate, and experiments yielding

EC<sub>50</sub> < 0.5  $\mu\text{M}$  were repeated at least once. For assays to test the role of the gatekeeper residue, the above procedure was followed except that three *T. gondii* cell lines expressing  $\beta$ -galactosidase in a "wild type" background (as above in the standard assay) or also expressing HA-TgCDPK1 or HA-Gly128Met TgCDPK1 were assayed in parallel.

## ■ ASSOCIATED CONTENT

### ☛ Supporting Information

Tabulation of IC<sub>50</sub>-fold differences between human kinases and TgCDPK1; graphical comparison of SRC and TgCDPK1 enzymatic IC<sub>50</sub> results; Tg cell proliferation EC<sub>50</sub> shifts with Gly128Met TgCDPK1 mutant for compounds **15o** and **16n**; synthesis and characterization data for all compounds. This material is available free of charge via the Internet at <http://pubs.acs.org>.

### Accession Codes

<sup>†</sup>The PDB code for the X-ray crystallographic structure of compound **15n** bound to wild type *T. gondii* CDPK1 is 3SX9.

## ■ AUTHOR INFORMATION

### Corresponding Author

\*For W.C.V.V.: phone, 206-543-2447; fax, 206-616-4898; e-mail, [wesley@uw.edu](mailto:wesley@uw.edu). For D.J.M.: phone, 206-543-1653; fax, 206-685 7002; e-mail, [maly@chem.washington.edu](mailto:maly@chem.washington.edu).

### Notes

The authors declare no competing financial interest.

## ■ ACKNOWLEDGMENTS

We are grateful for the technical assistance of Suzanne Scheele from the Parsons lab. This work was funded by the National Institute of General Medical Sciences Grant R01GM086858 (D.J.M.) and the National Institute of Allergy and Infectious Diseases Grants R01AI080625 (W.C.V.V.) and R01AI067921 (E.A.M. and W.C.V.V.). J.A.G. was supported by a training grant from the National Institute of Allergy and Infectious Diseases (Grant T32AI007509). The authors are solely responsible for the content.

## ■ ABBREVIATIONS USED

ATP, adenosine triphosphate; Boc, *tert*-butyloxycarbonyl; CDPK1, calcium-dependent protein kinase 1; CSK, C-terminal SRC kinase; DIAD, diisopropyl azodicarboxylate; DME, dimethoxyethane; EC<sub>50</sub>, half-maximal effective concentration; EGFR, epidermal growth factor receptor kinase; EPHA3, EPH receptor A3 kinase; IC<sub>50</sub>, half-maximal inhibitory concentration; LCK, lymphocyte-specific protein tyrosine kinase; TBDMS, *tert*-butyldimethylsilyl

## ■ REFERENCES

- (1) Tenter, A. M.; Heckerth, A. R.; Weiss, L. M. *Toxoplasma gondii*: from animals to humans. *Int. J. Parasitol.* **2000**, *30*, 1217–1258.
- (2) Schwartzman, J. D.; Maguire, J. H. *Toxoplasmosis*. In *Tropical Infectious Diseases: Principles, Pathogens and Practice*, 3rd ed.; W. B. Saunders: Edinburgh, U.K., 2011; Chapter 103, pp 722–728.
- (3) Jones, J. L.; Muccioli, C.; Belfort, R. Jr.; Holland, G. N.; Roberts, J. M.; Silveira, C. Recently acquired *Toxoplasma gondii* infection, Brazil. *Emerging Infect. Dis.* **2006**, *12*, 582–587.
- (4) Demar, M.; Hommel, D.; Djossou, F.; Peneau, C.; Boukhari, R.; Louvel, D.; Bourbigot, A. M.; Nasser, V.; Ajzenberg, D.; Darde, M. L.; Carne, B. Acute toxoplasmoses in immunocompetent patients hospitalized in an intensive care unit in French Guiana. *Clin. Microbiol. Infect.* [Online early access]. DOI: 10.1111/j.1469-0691.2011.03648.x. Published Online: September 29, 2011.

(5) Silveira, C.; Vallochi, A. L.; Rodrigues da Silva, U.; Muccioli, C.; Holland, G. N.; Nussenblatt, R. B.; Belfort, R.; Rizzo, L. V. *Toxoplasma gondii* in the peripheral blood of patients with acute and chronic toxoplasmosis. *Br. J. Ophthalmol.* **2011**, *95*, 396–400.

(6) Pappas, G.; Roussos, N.; Falagas, M. E. Toxoplasmosis snapshots: global status of *Toxoplasma gondii* seroprevalence and implications for pregnancy and congenital toxoplasmosis. *Int. J. Parasitol.* **2009**, *39*, 1385–1394.

(7) Jones, J. L.; Kruszon-Moran, D.; Sanders-Lewis, K.; Wilson, M. *Toxoplasma gondii* infection in the United States, 1999–2004, decline from the prior decade. *Am. J. Trop. Med. Hyg.* **2007**, *77*, 405–410.

(8) Yolken, R. H.; Torrey, E. F. Are some cases of psychosis caused by microbial agents? A review of the evidence. *Mol. Psychiatry* **2008**, *13*, 470–479.

(9) Dubey, J. P.; Jones, J. L. *Toxoplasma gondii* infection in humans and animals in the United States. *Int. J. Parasitol.* **2008**, *38*, 1257–1278.

(10) Montoya, J. G.; Liesenfeld, O. Toxoplasmosis. *Lancet* **2004**, *363*, 1965–1976.

(11) Montoya, J. G.; Remington, J. S. Management of *Toxoplasma gondii* infection during pregnancy. *Clin. Infect. Dis.* **2008**, *47*, 554–566.

(12) Nagamune, K.; Sibley, L. D. Comparative genomic and phylogenetic analyses of calcium ATPases and calcium-regulated proteins in the apicomplexa. *Mol. Biol. Evol.* **2006**, *23*, 1613–1627.

(13) Lourido, S.; Shuman, J.; Zhang, C.; Shokat, K. M.; Hui, R.; Sibley, L. D. Calcium-dependent protein kinase 1 is an essential regulator of exocytosis in *Toxoplasma*. *Nature* **2010**, *465*, 359–362.

(14) Kieschnick, H.; Wakefield, T.; Narducci, C. A.; Beckers, C. *Toxoplasma gondii* attachment to host cells is regulated by a calmodulin-like domain protein kinase. *J. Biol. Chem.* **2001**, *276*, 12369–12377.

(15) Ojo, K. K.; Larson, E. T.; Keyloun, K. R.; Castaneda, L. J.; Derocher, A. E.; Inampudi, K. K.; Kim, J. E.; Arakaki, T. L.; Murphy, R. C.; Zhang, L.; Napuli, A. J.; Maly, D. J.; Verlinde, C. L.; Buckner, F. S.; Parsons, M.; Hol, W. G.; Merritt, E. A.; Van Voorhis, W. C. *Toxoplasma gondii* calcium-dependent protein kinase 1 is a target for selective kinase inhibitors. *Nat. Struct. Mol. Biol.* **2010**, *17*, 602–607.

(16) Murphy, R. C.; Ojo, K. K.; Larson, E. T.; Castellanos-Gonzalez, A.; Perera, B. G.; Keyloun, K. R.; Kim, J. E.; Bhandari, J. G.; Muller, N. R.; Verlinde, C. L.; White, A. C. Jr.; Merritt, E. A.; Van Voorhis, W. C.; Maly, D. J. Discovery of potent and selective inhibitors of calcium-dependent protein kinase 1 (CDPK1) from *C. parvum* and *T. gondii*. *ACS Med. Chem. Lett.* **2010**, *1*, 331–335.

(17) Bulawa, C. E.; Devit, M.; Elbaum, D. Preparation of Pyrazolopyrimidinamines as Modulators of Protein Trafficking. WO2009062118A2, 2009.

(18) Larson, E. T.; Ojo, K. K.; Murphy, R. C.; Johnson, S. M.; Zhang, Z.; Kim, J. E.; Leibly, D. J.; Fox, A. M. W.; Reid, M. C.; Dale, E. J.; Perera, B. G. K.; Kim, J.; Hewitt, S. N.; Hol, W. G. J.; Verlinde, C. L. M. J.; Fan, E.; Van Voorhis, W. C.; Maly, D. J.; Merritt, E. A. Unpublished results.

(19) Bain, J.; Plater, L.; Elliott, M.; Shpiro, N.; Hastie, C. J.; McLauchlan, H.; Klevernic, I.; Arthur, J. S.; Alessi, D. R.; Cohen, P. The selectivity of protein kinase inhibitors: a further update. *Biochem. J.* **2007**, *408*, 297–315.

(20) Hanke, J. H.; Gardner, J. P.; Dow, R. L.; Changelian, P. S.; Brissette, W. H.; Weringer, E. J.; Pollok, B. A.; Connelly, P. A. Discovery of a novel, potent, and Src family-selective tyrosine kinase inhibitor. Study of Lck- and FynT-dependent T cell activation. *J. Biol. Chem.* **1996**, *271*, 695–701.

(21) Liu, Y.; Bishop, A.; Witucki, L.; Kraybill, B.; Shimizu, E.; Tsien, J.; Ubersax, J.; Blethrow, J.; Morgan, D. O.; Shokat, K. M. Structural basis for selective inhibition of Src family kinases by PP1. *Chem. Biol.* **1999**, *6*, 671–678.

(22) Seeber, F.; Boothroyd, J. C. *Escherichia coli* beta-galactosidase as an in vitro and in vivo reporter enzyme and stable transfection marker in the intracellular protozoan parasite *Toxoplasma gondii*. *Gene* **1996**, *169*, 39–45.